

## Anomalous frequency pulling in the photorefractive oscillators

Ramon Herrero\* and Daniel Hennequin

*Laboratoire de Physique des Lasers, Atomes et Molécules, Unité mixte du Centre National de la Recherche Scientifique, Centre d'Etudes et de Recherches Lasers et Applications, Bâtiment P5, Université des Sciences et Technologies de Lille, F-59655 Villeneuve d'Ascq Cedex, France*

(Received 22 February 1999)

The emission frequency of an optical oscillator is not, in general, the cavity frequency, because it results from a compromise between the cavity and the material (atom, crystal) frequencies: this phenomenon is known as frequency pulling. We study in this paper the mechanisms leading to frequency pulling in oscillators with photorefractive gain (OPG), and compare them with those of lasers. We find that because the pulling in OPG does not depend explicitly on the empty cavity mode frequency, behaviors different from those observed in lasers are obtained. In particular, for a given set of parameters, the frequency pulling has a constant sign, so that the emission frequency is always larger (or smaller) than the maximum gain frequency. This leads to the counterintuitive effect that, in some conditions, the emitted intensity could decrease as the losses are decreased. [S1050-2947(99)09908-4]

PACS number(s): 42.65.Hw, 42.70.Nq

### I. INTRODUCTION

In the field of spatiotemporal dynamics and transverse pattern formations in active systems, studies have been realized not only on lasers but also on oscillators with photorefractive gain (OPG) [1–6]. The latter presents the main advantage of very long characteristic times, leading to dynamics in the range of a few hertz. This simplifies greatly the detection and the analysis of the spatiotemporal dynamics. OPG are used in many other fields, as they offer good properties for pattern recognition devices, mass memories, and image processing [7]. In spite of a gain process fundamentally different, large analogies between lasers and OPG have been emphasized, leading, e.g., to model the OPG as a class-A laser [8].

However, deep differences exist in the involved processes, in particular in the frequency domain. Indeed, because of its very narrow gain bandwidth (only a few Hz), the OPG emits always at the same frequency (within a few hertz), and, therefore, a huge frequency pulling is required for oscillation. We show in this paper that these properties lead to some original behaviors of the OPG, fundamentally different from that of the laser. We show in particular that a decrease of the losses may lead to a decreasing of the emitted intensity, and that frequency pulling can take values larger than the frequency interval between transverse modes. We give in this paper experimental evidence of these atypical behaviors.

The paper is organized as follows: after this introduction, the second part is devoted to the description of the experimental setup. The third part derives some properties of the frequency pulling in the OPG from a model previously developed [9]. Finally, Sec. IV describes the experimental observations and their interpretation as a consequence of the properties described in Sec. III.

### II. EXPERIMENTAL SETUP

The photorefractive oscillator is constituted by a ring cavity (length  $L = 1.34$  m) with a BSO ( $\text{Bi}_{12}\text{SO}_{20}$ ) photorefractive crystal as an amplifier. The cavity is limited by three plane mirrors and a beam splitter with 90% reflection, used as an external coupler (Fig. 1). We used a cavity with four mirrors because it corresponds to a simpler distribution of cavity eigenmodes (in a cavity with an odd number of mirrors, a geometrical phase introduces a dependence of the mode frequency on the mode symmetry). The cavity is stabilized by a lens (focal length  $f = 1$  m), and its transverse size is ruled by an iris. The beam waist ( $w_0 = 0.4$  mm) is located inside the crystal, and the distance between the iris and the crystal is small in comparison with the Rayleigh

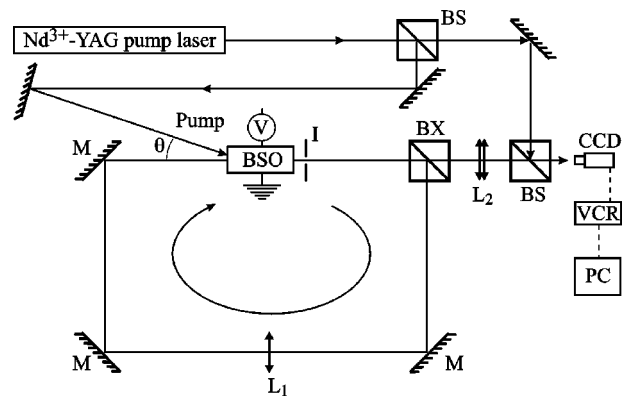


FIG. 1. Experimental setup. The cavity is limited by the mirrors  $M$  and the beam splitter  $BX$ .  $L_1$  is a lens that geometrically stabilizes the cavity, while the iris  $I$  rules the Fresnel number. The angle  $\theta = 1.5^\circ$  between the pump and the cavity axis has been chosen to optimize the gain.  $L_2$  is a set of lens to image the pattern on the CCD camera. The pictures are recorded on a video recorder (VCR) and/or processed on a computer (PC). A voltage  $V$  is applied on the crystal to increase the gain. The other beam splitters (BS) allow us to make interferences between the intracavity signal and the pump, in order to perform a heterodyne detection.

\*Present address: Dept. de Física, Universitat Autònoma de Barcelona, E-08193 Bellaterra, Spain.

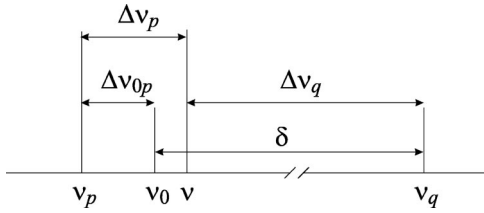


FIG. 2. Illustration of the different frequencies involved in the OPG.  $\nu_p$  is the pump frequency and  $\nu_0$  the maximum gain frequency.  $\nu_q$  is the empty cavity mode frequency, while  $\nu$  is the active frequency corresponding to  $\nu_q$ .

length (typically 8 cm against 94 cm), so that the iris is in the near field area. The gain in the BSO crystal is obtained by two-wave mixing with a pump beam provided by a frequency doubled Nd<sup>3+</sup>-YAG laser (wavelength  $\lambda = 532$  nm, intensity about 10 mW/cm<sup>2</sup>): the optical grating created by interference between the pump beam and the intracavity beam induces an electric charge grating, which itself induces an index grating with a phase shift  $\phi$  with the optical grating. The maximum gain is obtained for  $\phi = \pi/2$ . In the BSO, phase-shift value is adjusted with a dc electric field applied to the crystal. Therefore, the gain is linearly related with the applied electric field, which can reach 1 kV/mm in our experiments, corresponding to a typical linear gain of 10. Note that the gain curve is detuned from the pumping frequency  $\nu_p$ : the maximum gain frequency  $\nu_0$  is such that  $\Delta\nu_{0p} = \nu_0 - \nu_p$  takes values between 1 and 4 Hz, depending on the pump power (Fig. 2). At the startup of the oscillator, the intracavity beam intensity  $I_s$  is zero except for the diffusion of the pump in the crystal. Thus the signal is constructed from this diffusion noise.

The signal pattern emitted by such an oscillator can be interpreted through the eigenmodes of the empty cavity, namely the Hermite-Gauss (HG) or the Laguerre-Gauss (LG) modes [1]. Each mode is associated with its longitudinal index  $k$  and its transverse indices  $m$  and  $n$  (respectively,  $p$ ,  $l$ , and  $i$ ) for HG (respectively, LG) modes. In the following, HG (respectively, LG) modes will be noted  $H_{mn}$  (respectively,  $A_{pli}$ ). The frequency separation between two modes with successive  $k$  and identical transverse indices is the free spectral range  $\Delta\nu_L = c/L$ , where  $c$  is the light velocity. The frequency of a transverse mode is ruled by the family index  $q = m + n$  (respectively,  $q = 2p + l$ ) for HG (respectively, LG) modes. The frequency separation between two modes with successive  $q$  and same  $k$  is  $\Delta\nu_T = \Delta\nu_L / \pi \arccos \sqrt{1 - L/2f}$ . The ratio  $R_\nu = \Delta\nu_L / \Delta\nu_T$  plays a main role in the dynamics of the oscillator and may be adjusted by changing  $L$  or  $f$ . Note that astigmatism changes the frequency of modes and, therefore, lifts the degeneracy of modes with same  $q$ . Because of the high level of losses in the cavity (typically 75% by round trip), the resonance width of each mode, i.e., the cavity linewidth  $\Delta\nu_C$ , is very large:  $\Delta\nu_C \approx 50$  MHz.

As modes with higher  $q$  are more spatially extended, the modes effectively emitted by the oscillator depend on its transverse size. This size, fixed by the iris inserted in the cavity, is measured through the Fresnel number  $N_F$ , with

$$N_F = \left( \frac{a}{w_a} \right)^2,$$

where  $a$  is the iris aperture and  $w_a$  is the beam size at the iris ( $w_a \approx w_0$ ). In our cavity,  $N_F$  may take values up to 150, but we focus here on small values, typically up to 30.

The gain bandwidth  $\Delta\nu$  of the OPG is only a few Hz, leading to dynamics time scale of the order of 1 s. Therefore, the detection of the spatial patterns may be done through a standard video camera.

The long time scale of the acquisition processes makes primordial the stability of the cavity. To realize the experiments described here, we have used an active stabilization of the cavity: a counterpropagating control beam with an intensity  $10^2$  to  $10^3$  smaller than the main signal beam and with normal field polarization as compared to the latter is introduced in the cavity. This control beam interferes with a reference beam, leading to an interference pattern monitoring the cavity length. A lock-in amplifier is then used to generate an error signal that compensates for the fluctuations of the cavity length by moving one of the mirrors of the cavity through a piezoelectric translator. The control beam comes from the pump laser, so that the possible frequency shift of the later is also compensated.

It is easy with such a system to measure the emission frequency  $\nu$  or the phase of the fields. A heterodyne detection is achieved by mixing the pump and the intracavity signals. If the pump field phase is taken as a reference, the resulting field is

$$E_r(x, y, t) = E_p(x, y) e^{i2\pi\nu_p t} + E(x, y) e^{i2\pi\nu t} e^{i\varphi} \quad (1)$$

leading to a detected intensity:

$$I_r = I_p + I + 2E_p E \cos[2\pi(\nu - \nu_p)t + \varphi], \quad (2)$$

where  $E_p$  and  $E$  (respectively,  $I_p$  and  $I$ ) are the pump and intracavity fields (respectively, intensities), while  $\varphi$  is the phase of the intracavity field. It appears from Eq. (2) that the time-dependent part of the intensity provides the frequency difference between the pump and intracavity signal frequencies, while the phase of the intracavity field can be deduced from snapshots of the interference pattern.

### III. FREQUENCY PULLING

As the gain bandwidth of the OPG is very narrow, its emission frequency always remains within a few hertz of the maximum gain frequency  $\nu_0$ , whatever the cavity length. This can be obtained if, as in lasers, frequency pulling shifts the emission frequency  $\nu$  from the empty cavity mode frequency  $\nu_q$  in the direction of  $\nu_0$  (Fig. 2). However, this frequency pulling plays here a much more important role than in lasers, as  $\nu$  is very close to  $\nu_0$ . Let us remember that in lasers, the relation between the effective emission frequency  $\nu$  of a mode and the empty cavity mode frequency  $\nu_q$  is given by

$$\nu - \nu_q = (\nu_0 - \nu_q) \Delta\nu_C / \Delta\nu, \quad (3)$$

where  $\Delta\nu_C$  and  $\Delta\nu$  are, respectively, the cavity and gain linewidth. Note that if this expression was applied to the OPG, we would find a large frequency pulling, since experi-

mentally, values of  $\Delta\nu_C$  are very large. However, previous theoretical works show that frequency pulling in the OPG is given by [9]

$$\Delta\nu_q = \nu - \nu_q = \frac{1}{2t_d} \frac{C_q}{S_q}, \quad (4)$$

with

$$C_q = \int_0^l dz F(z) \cos[\psi_q(z) - \psi_q(0) + \phi], \quad (5a)$$

$$S_q = \int_0^l dz F(z) \sin[\psi_q(z) - \psi_q(0) + \phi], \quad (5b)$$

$$F(z) = \frac{I_0(z) \sqrt{I_q(z)}}{I_0(z) + f_q I_q(z)}. \quad (5c)$$

$t_d$  is the cavity lifetime and  $l$  is the length of the crystal. The  $z$  axis is the propagation axis, with its origin at the input of the crystal.  $I_0$  and  $I_q$  are, respectively, the pump beam intensity and the  $q$ -mode intracavity intensity.  $\psi_q(z)$  is the phase of the  $q$ -mode electric field while  $f_q$  is a constant, which depends on the transverse profile of the mode. In the following, we will use  $f_q = 1$  for simplicity, as we discuss essentially the monomode case and because the profile beam shape does not change the qualitative behavior of the OPG. For the sake of clarity in the following discussion,  $\Delta\nu_q$  is normalized to the free spectral range,

$$\overline{\Delta\nu_q} = \frac{\Delta\nu_q}{\Delta\nu_L} = \frac{\mathcal{P}}{2} \frac{C_q}{S_q}, \quad (6)$$

where  $\mathcal{P}$  is the cavity loss coefficient.

The main—and most surprising—characteristics of Eq. (6) is that frequency pulling in OPG appears not to depend explicitly on the frequency of the empty cavity mode, or on the maximum gain frequency of the crystal, but only on the intensity and phase of pump and mode  $q$ . This is a fundamental difference of OPG with lasers. In the latter, the frequency pulling vanishes as the cavity detuning  $\delta = \nu_q - \nu_0$  goes to zero, and it increases as  $\delta$  increases: frequency pulling always reduces  $|\nu - \nu_0|$ . In the former, as frequency pulling does not depend on cavity detuning, its action on  $|\nu - \nu_0|$  cannot be directly predicted. However, it appears in Eqs. (4) and (5) that in the OPG,  $\Delta\nu_q$  depends on the pump and mode intensities, and on the mode phase. Moreover, the phase  $\psi_q(z)$  is essentially proportional to  $I_q(z)/I_q(0)$  [9] and  $I_q(z)$  is related to  $I_q(0)$ . Therefore, all parameters being fixed,  $\Delta\nu_q$  appears to depend exclusively on the mode intensity  $I_q(0)$ . From this relation, it is possible to evaluate the active frequency as a function of the detuning. In the next paragraphs, we derive this relation and some other fundamental properties of OPG emission mechanisms.

We use the approximations proposed in [9]. The first one concerns the space evolution of the intensities in the crystal. Introducing as in [9] the lossless intensities  $I_{0,q}(z) = \bar{I}_{0,q}(z) e^{-\alpha z}$ , where  $\alpha$  is the absorption coefficient in the photorefractive crystal, we assume that the sum of the pump

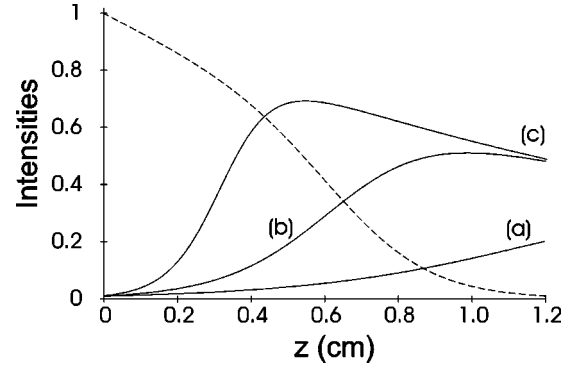


FIG. 3. Theoretical evolution of intensities in the crystal. The solid lines (dashed line) represent the evolution of  $I_q(z)$  [ $I_0(z)$ ]. The gain is (a)  $\Gamma = 5 \text{ cm}^{-1}$ , (b)  $\Gamma = 10 \text{ cm}^{-1}$ , and (c)  $\Gamma = 20 \text{ cm}^{-1}$ . Other parameters are  $\phi = \pi/4$ ,  $\alpha = 0.6 \text{ cm}^{-1}$ ,  $I_q(0) = 0.01$ , and  $\Gamma = 10 \text{ cm}^{-1}$  for  $I_0(z)$ .

and mode lossless intensities is a constant all along the crystal, and we normalize this sum to 1:

$$\bar{I}_0(z) + \bar{I}_q(z) = 1. \quad (7)$$

This leads to the following equation for the mode intensity [9]:

$$\frac{d\bar{I}_q(z)}{dz} = \eta \bar{I}_q(z) [1 - \bar{I}_q(z)] \quad (8)$$

with  $\eta = \Gamma \sin \phi$ , where  $\Gamma$  is the crystal gain at the active frequency  $\nu$ . Thus the space evolution of the intensities in the crystal can be approximated by

$$I_q(z) = \frac{I_q(0)}{I_q(0) + [1 - I_q(0)] \exp(-\eta z)} \exp(-\alpha z), \quad (9a)$$

$$I_0(z) = \exp(-\alpha z) - I_q(z). \quad (9b)$$

Concerning the phase evolution, [9] shows that it can be approximated by

$$\psi_q(z) - \psi_q(0) = \frac{\eta'}{\eta} \ln \left( \frac{\bar{I}_q(z)}{\bar{I}_q(0)} \right) \quad (10)$$

with  $2\eta' = \Gamma \cos \phi$ . Figure 3 shows the typical evolution of intensities inside the crystal, as a function of  $z$ , obtained with Eq. (9), for different values of the gain  $\Gamma$ . Note that in these equations, the independent variable  $z$  is rescaled by a factor  $\cos \theta$ , where  $2\theta$  is the angle between the pump and mode beams, typically  $2.6 \times 10^{-2}$  rad. Thus  $\cos \theta$  is almost equal to 1. Other parameters are typical of our experiments (see caption of the figure). For a given gain  $\Gamma$ , the value of  $I_q(0)$  determines that of  $I_q(l)$ , and, therefore, the net gain  $\gamma_n = I_q(l)/I_q(0)$  of the crystal. In stationary regime,  $\gamma_n$  must compensate exactly for the cavity losses [ $\gamma_n(1 - \mathcal{P}) = 1$ ], and each value of  $I_q(0)$  corresponds to a unique value of the gain. Using Eq. (9a) in the expression of  $\gamma_n$ , we obtain

$$\Gamma = - \frac{1}{l \sin \phi} \ln \left( \frac{I_q(0) - I_{\max}}{I_q(0) - 1} \right) \quad (11)$$

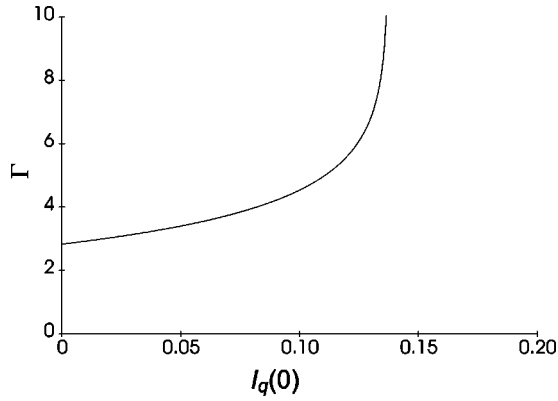


FIG. 4. Theoretical gain value  $\Gamma$  necessary to obtain  $I_q(0)$  at the crystal input. Parameters are  $\phi = \pi/4$  and  $\mathcal{P} = 75\%$ .

with

$$I_{\max} = \frac{\exp(-\alpha l)}{\gamma_n}. \quad (12)$$

Figure 4 shows the gain value necessary to obtain an intensity  $I_q(0)$  with 75% cavity losses, as in our cavity. The intensity grows with the gain, but intensities larger than  $I_{\max}$  cannot be obtained. In this last case, the pump intensity is not sufficient to generate the energy exchange necessary to reach  $I_q(l)$ . On the other hand, the effective gain  $\Gamma$  of the crystal depends critically on the active frequency, typically as [9–11]

$$\Gamma(\nu) = \frac{1}{\Gamma_0^{-1} + (a_p \Delta \nu_p)^{-1} (1 - \Delta \nu_p / \Delta \nu_{0p})^2}, \quad (13)$$

where  $\Delta \nu_p = \nu - \nu_p$ ,  $\Gamma_0$  is the maximum gain (i.e., the gain at  $\nu_0$ ), and  $a_p$  is the slope of the curve at  $\nu = \nu_p$ .  $a_p$ ,  $\Gamma_0$ , and  $\nu_0$  depend mainly on the crystal characteristics and the angle between the pump beam and the cavity axis. Therefore, expressions (11) and (13) link the emission frequency with the emission intensity, in an asymmetrical way, as shown in Fig. 5. This asymmetry is inherent to that of the gain as a function of the emission frequency. Through Fig. 5 we have now the relation between the active frequency of the oscillator and its

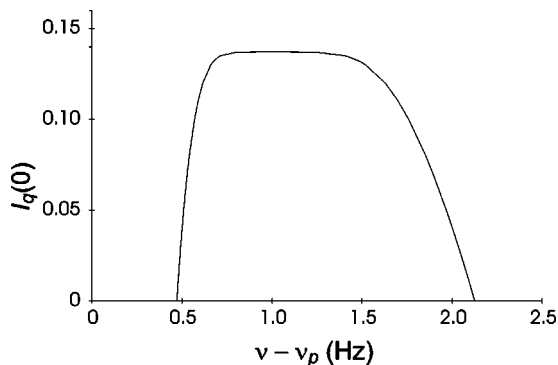


FIG. 5. Output intensity of the OPG as a function of the active frequency. Parameters are  $\phi = \pi/4$ ,  $\mathcal{P} = 75\%$ ,  $\alpha = 0.6 \text{ cm}^{-1}$ ,  $\Gamma_0 = 10 \text{ cm}^{-1}$ ,  $\Delta \nu_{0p} = 1 \text{ Hz}$ , and  $a_p = 2$ . The three previous parameters have been obtained by fitting an experimental curve of the gain as a function of the frequency.

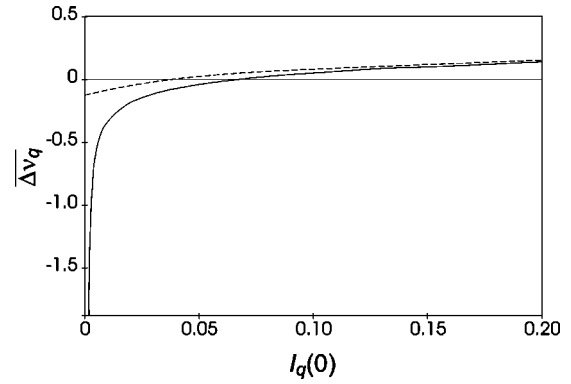


FIG. 6. Plot of the frequency pulling  $\Delta \nu_q$  as a function of the intensity  $I_q(0)$  in the cavity. Solid (dashed) line corresponds to  $\Gamma = 10 \text{ cm}^{-1}$  ( $5 \text{ cm}^{-1}$ ). Other parameters are those of Fig. 3.

emission intensity. This relation has been obtained using the properties of the crystal and the relation of self-consistence of the field inside the cavity.

Let us now come back to the mechanism of frequency adjustment in the OPG. Figure 6 shows a plot of  $\Delta \nu_q$  as a function of  $I_q(0)$  obtained by using Eqs. (6), (9), and (10). This curve does not correspond to the stationary regime of the OPG, because the gain  $\Gamma$  has been fixed, while the real gain depends on the intensity, as we have seen in Eq. (11). However, this curve already shows a crucial property of the frequency pulling in OPG: the zero frequency pulling does not correspond to the maximum intensity, and the curve of detuning as a function of intensity is completely asymmetric: positive (negative) frequency pulling corresponds to large (small) intensities. Let us give a first analysis of the mechanisms leading to oscillation in an OPG. For a given cavity detuning  $\delta_q$ , a necessary condition to have a significant gain is a frequency pulling of  $\Delta \nu_q \approx \delta$ , because the gain linewidth is very narrow. Following Fig. 6, this value corresponds to a unique intensity  $I_q(0)$ . In the stationary regime, this intensity must correspond to a gain compensating exactly the cavity losses. Therefore, the stationary regime appears to result from a self-adjustment of the intensity with the cavity detuning. This adjustment can occur only via an adjustment of the gain, i.e., of the  $\nu - \nu_0$  value.

To obtain the dependence of the active frequency with the detuning, we inject the equations corresponding to Fig. 5 in those corresponding to Fig. 6. The result is shown in Fig. 7 for two different values of  $\phi$ . We see that one can define an *active detuning interval*, i.e., a detuning interval on which the OPG oscillates: for detuning values inside this interval, two active frequencies are compatible with oscillation. Outside it, the corresponding cavity mode cannot oscillate, because the necessary pulling does not correspond to a reachable intensity (e.g., the required gain is too large). The parameter  $\phi$  appears to be critical, but only concerning the width of the active detuning interval. For example,  $\phi = 0.3$  corresponds to a value relatively closer from a singularity (as described in [9]) than  $\phi = \pi/4$ , and the active detuning interval is larger. The choice between the two possible active frequencies results from a stability criterion. Introducing the gain dependence on the intensity [Eq. (11)] in Fig. 6, we obtain the real variation of  $\Delta \nu_q$  with  $I_q(0)$  (Fig. 8). The stability of the active frequency  $\nu$  can be deduced through

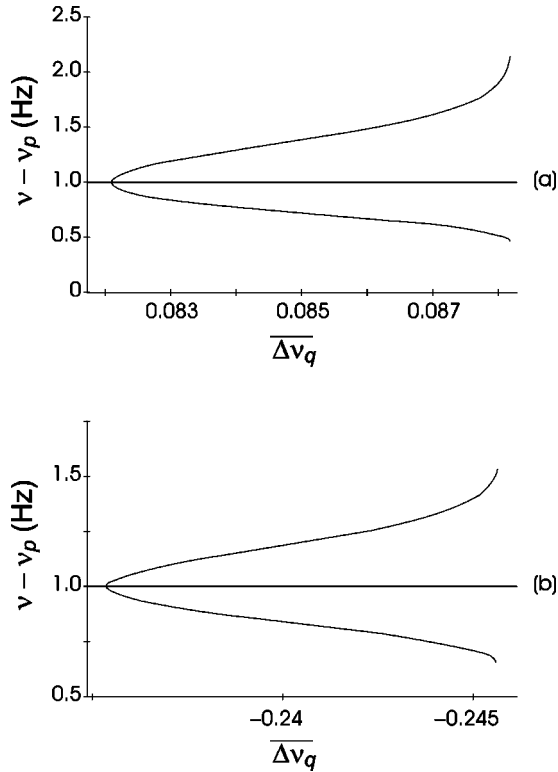


FIG. 7. Plot of the active frequency  $\nu'_q$  as a function of the frequency pulling. Note that in the stationary regime, frequency pulling is almost equal to detuning, and, therefore, these curves give also the dependence of  $\nu'_q$  with  $\delta$ . The phase is  $\Phi = \pi/4$  and  $\Phi = 0.3$  in (a) and (b), respectively. Other parameters are those of Fig. 3.

Fig. 8 and Fig. 5: considering perturbations of a given frequency, the successive iterations between both figures show an amplification (unstable case) or an attenuation (stable case) of the perturbation. Lower (higher) frequencies than  $\nu_0$  appear to be stable (unstable) for the  $\phi = \pi/4$ . This result is general for  $0 < \phi < \pi/2$ , while for  $\pi/2 < \phi < \pi$  lower (higher) frequencies than  $\nu_0$  are unstable (stable). For  $\pi < \phi < 2\pi$ , the gain is negative. Moreover the frequency pulling is negative for  $0 < \phi < \phi_1$  and  $\pi/2 < \phi < \phi_2$  and positive for  $\phi_1 < \phi < \pi/2$  and  $\phi_2 < \phi < \pi$ , where  $\phi_1$  and  $\phi_2$  depend on the OPG parameters. In this way, the frequency pulling in OPG oscillators appears to be totally different from those of lasers. First, the resonance is not particularly favorable to the oscillation. It is the gain value rather than the detuning that fixes

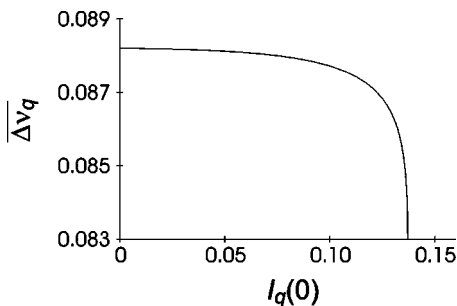


FIG. 8. Frequency pulling  $\overline{\Delta\nu_q}$  as a function of  $I_q(0)$ . In this figure, contrary to the plot of Fig. 6, the gain is not fixed, but takes its real value depending on  $I_q(0)$ . Parameters are those of Fig. 6.

the frequency range in which the OPG oscillates and a spectacular consequence is that frequency pulling has a fixed sign, depending only on the  $\phi$  angle. Another consequence is that the active detuning interval does not contain *a priori*  $\nu_0$ , and so when several modes are competing, the oscillating one is not *a priori* the most resonant one.

We found in the above paragraph that monomode theory predicts very unusual properties for frequency pulling in an OPG, namely, an asymmetry in the emission intensity as a function of the detuning, and a constant sign frequency pulling. We describe in the following some experimental observations confirming these theoretical results. Some properties of the multimode behavior are also experimentally studied. We show in particular that the properties of frequency pulling in OPG can lead to surprising behavior, as, e.g., a decreasing of the output intensity of the OPG while the losses are decreased.

#### IV. EXPERIMENTAL RESULTS

The present experiments have been realized with the cavity described above, corresponding to  $\Delta\nu_L = 224$  MHz and  $R_\nu \approx 3$ . In this case, as the cavity detuning  $\delta = \nu_q - \nu_0$  is swept, three zones are successively encountered, where modes with  $q = 3n$ ,  $q = 3n + 1$ , and  $q = 3n + 2$  ( $n$  is a integer) are resonant. When the Fresnel number is high enough, these zones first join, and then mix together [1]. At a low Fresnel number, typically  $N_F \lesssim 3$ ; only  $q = 0$ ,  $q = 1$ , and  $q = 2$  families are encountered. Thanks to the choice of  $R_\nu \approx 3$ , the three families are separated by  $\Delta\nu_L/3$ , which is the maximum frequency separation allowed for these mode families, making easier the analysis as a function of the frequency. For a given mode family, as  $\delta$  is varied, the total intensity of the pattern first grows, reaches a maximum, decreases, and finally vanishes. An example of such an evolution is given in Fig. 9(a) for the  $q = 1$  family: the asymmetry theoretically predicted appears clearly. The  $\delta$  origin is arbitrarily chosen at the maximum of the curve. Note that for technical reasons, the asymmetry is smoothed: because our active stabilization of the cavity is less efficient when the detuning is swept, we had to record these curves in a relatively short time (typically 30 s), so that the growing edge of the curve appears less stiff than it really is.

Figure 9(b) shows the way the beam frequency evolves on the same interval. The frequency origin is chosen at the maximum signal frequency  $\nu_0$ , in this particular case at 1.37 Hz from  $\nu_p$ , while the  $\delta$  origin is the same as in Fig. 9(a). It appears on this example that as  $\delta$  is tuned, the beam frequency grows from  $\nu_{\min} \approx 0$  Hz (i.e., 1.37 Hz from  $\nu_p$ ) to  $\nu_{\max} \approx +1$  Hz (i.e., 2.37 Hz from  $\nu_p$ ). Thus not only the emission frequency exhibits a severe asymmetry when the frequency cavity is tuned, but also the frequency appears to be always on the opposite side of  $\nu_0$  as compared to  $\nu_p$ . This behavior agrees with the results deduced from Figs. 7 and 8. It appears whatever the direction of the detuning variation, and is general in the present experimental setup. In our observations, the emission frequency is sometimes between  $\nu_p$  and  $\nu_0$ , sometimes on the other side of  $\nu_0$ . This depends on several parameters, as the cavity length, the crystal gain, or the angle  $2\theta$  between the pump and cavity beams. We have not found a simple rule to determine from these parameters

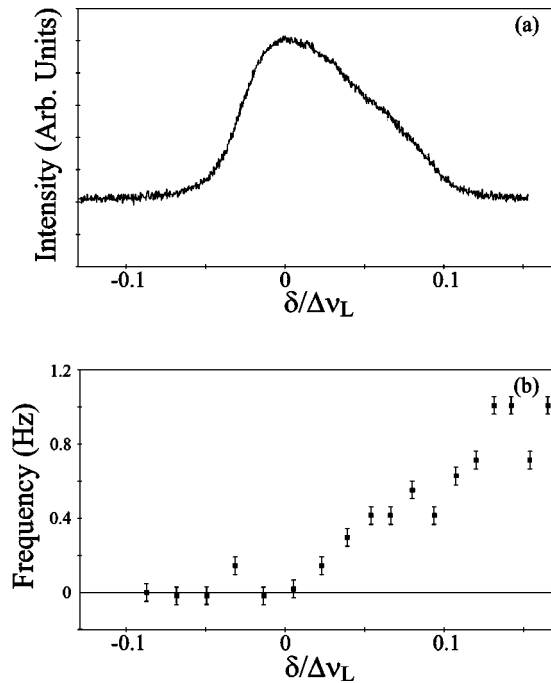


FIG. 9. Evolution of (a) the output intensity and (b) the emission frequency of the OPG as the cavity detuning is swept.  $\Delta\nu_L=196$  MHz and  $R_p=3$ . The pattern emitted is the  $q=1$  mode. The origins of detunings and frequencies are chosen at the resonance of the  $q=1$  mode.

on which side will be the frequency pulling, but this is not surprising as, from theoretical predictions, it depends on  $\phi$ , and this phase is not directly accessible in the experiments.

We showed in the theoretical section that as a consequence of the preceding results, when several modes are present, the oscillating mode is not necessarily the closest from  $\nu_0$ . We give in the following some observed behaviors resulting from this property. Let us look at what happens when for a given detuning, the Fresnel number is increased. In most cases, a mode appears as soon as the Fresnel number becomes large enough, and its intensity increases as a function of  $N_F$ . However, more complicated behaviors are ob-

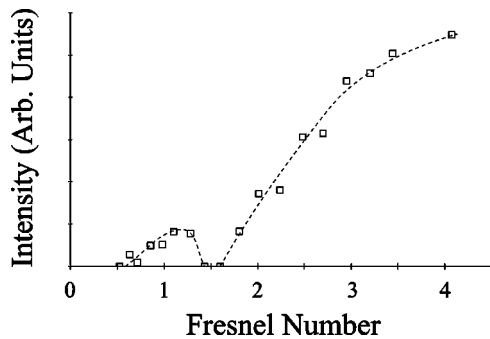


FIG. 10. Intensity emitted by the OPG as a function of the Fresnel number. Detuning is close to the maximum emission intensity of the  $q=2$  modes, slightly shifted towards the  $q=0$  emission area. Other parameters are that of Fig. 1. For  $0.5 < N_F < 1.1$ , the pattern is the  $H_{00}$  mode. Above  $N_F=1.6$ , the pattern is first the  $H_{02}$  mode, then transforms continuously in the  $A_{10}$  mode. The dashed lines do not result from a fit: they have been added to make easier the reading of the figure.

served, as illustrated in Fig. 10, obtained for the  $q=2$  family. The corresponding detuning is that of the maximum power emission of the  $q=2$  mode at  $N_F \geq 2$ , but shifted of some MHz (less than 10) in the direction of the  $q=0$  family. Without changing this cavity detuning, we increase the Fresnel number from 0 to 5 to obtain the diagram shown in Fig. 10, where the output intensity of the OPG is plotted as a function of the Fresnel number. The same behavior is observed when  $N_F$  is decreased (we did not observe any hysteresis). For  $N_F < 0.5$ , the diffraction losses are so high that no emission occurs. For  $0.5 < N_F < 1.1$ , the  $H_{00}$  mode appears and its intensity increases with the Fresnel number. As  $N_F$  is still increased, i.e., the losses are decreased, the  $H_{00}$  mode intensity decreases until, at  $N_F=1.4$ , it vanishes completely. Finally, at  $N_F=1.6$ , the oscillation starts again, but on the  $H_{02}$  mode. Further increasing the Fresnel number, the intensity of  $H_{02}$  increases, but is replaced progressively by the Laguerre-Gauss mode  $A_{10}$ . This behavior is quite unexpected in an optical oscillator: usually, the emission starts for a given Fresnel number, and then the intensity increases monotonically as the Fresnel number is increased.

To analyze this behavior, let us distinguish its different anomalies: (i) for  $N_F > 1.6$ , the intensity grows as a function of  $N_F$ , but the pattern changes progressively from  $H_{02}$  to  $A_{10}$  and (ii) while the detuning is fixed, the active mode depends on  $N_F$ : it is the  $q=2$  mode for high  $N_F$ , and the  $q=0$  mode for low  $N_F$ . Moreover, for  $1.1 < N_F < 1.6$ , the intensity of the OPG decreases, and even vanishes.

The first point (i) is easily explained by the presence of astigmatism, which lifts the frequency degeneracy of modes inside a family. If the  $H_{02}$  and  $H_{20}$  modes have not exactly the same frequency, the separation between the frequency of each mode and the gain frequency  $\nu_0$  is also different, and, therefore, one mode is favored as compared to the other one. When the diffraction losses become negligible, i.e., at a high Fresnel number, this difference no longer plays any role, and the Laguerre mode appears. More generally, if the Fresnel number is chosen larger than 3, modes of other families could also appear. Figure 11(a) shows what happens on a larger range of  $N_F$  in the case where the cavity detuning is chosen at the  $q=1$  family, but slightly shifted to the  $H_{00}$  mode. The mode appearing for  $N_F \geq 2.5$  can be either one of the HG modes or one of the LG modes, depending on the alignment of the cavity, and, therefore, on the astigmatism. When  $N_F$  becomes larger than 5, a saturation of the intensity is observed. More generally, after a Fresnel number whose value depends on the concerned mode family, the intensity could even decrease. This effect does not correspond to a decreasing of the emission power, but to a change in the spatial extension of the pattern, due to the appearance of new modes inside it. Moreover, when the Fresnel number is still increased, the patterns may become nonstationary. Figure 11(b) shows how the beam frequency evolves as a function of the Fresnel number. From  $N_F=2.5$ , it increases until  $N_F=5$ : the frequency pulling appears to depend on the Fresnel number. This behavior is also observed in lasers: when  $N_F$  increases, losses decrease, and, therefore,  $\Delta\nu_q$  decreases. In the present case, the mechanism is similar, as  $\Delta\nu_q$  depend implicitly from losses, through the self-consistence condition of the field after a round trip in the cavity. For  $N_F > 5$ , it is

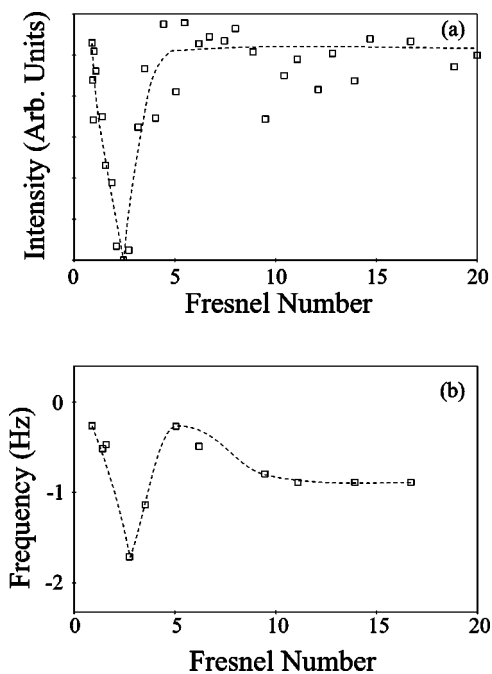


FIG. 11. Behavior of the OPG when cavity detuning is tuned close to the maximum emission intensity of the  $q=1$  modes, slightly shifted towards the  $q=0$  emission area. Other parameters are that of Fig. 1. In (a) intensity emitted by the OPG as a function of the Fresnel number and (b) frequency of the output beam as a function of the Fresnel number. Note that for Fresnel numbers larger than 10 the emitted pattern is made of several modes. The frequency indicated in the figure is in this case that corresponding to the wider mode. The dashed lines do not result from a fit: they have been added to make the reading of the figure easier.

more complicated to analyze the behavior as the system becomes multimode.

The second point (ii), i.e., the fact that different modes oscillate for the same detuning and different  $N_F$ , is typical from the OPG. It results from the fact that the active detuning interval depends on the cavity losses and, for modes with different shapes, from the parameter  $f_q$ . Therefore, when  $N_F$  is varied, this interval varies, and if the detuning is fixed, as in Fig. 10, different modes are successively observed. The decreasing of the intensity, and even the dark zone for  $1.4 < N_F < 1.6$ , are a consequence of that frequency shift of the active detuning interval. Figure 12 shows an enlargement of Fig. 10 with the corresponding emission frequencies (the points are not exactly the same as this is another set of experimental measurements): as  $N_F$  is increased,  $\nu - \nu_0$  first decreases as the pattern intensity increases. As  $N_F$  still increases, the pattern intensity starts to decrease, as described above, but  $\nu - \nu_0$  starts to increase. This means that starting from low  $N_F$ , the frequency pulling increases, the emission frequency  $\nu$  comes close to  $\nu_0$ , and then, as  $N_F$  is still increased,  $\nu$  goes farther from  $\nu_0$ . This behavior is deeply different from that observed in lasers: although the losses on mode  $H_{00}$  decrease, its intensity decreases and finally vanishes. As discussed in the previous section, this is well explained by the process of frequency pulling in the OPG: because the stationary regime results from a unique combination between the intensity and the frequency pulling, the intensity cannot take any value as the losses are decreased,

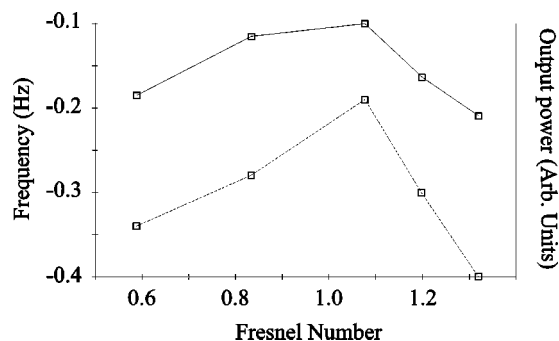


FIG. 12. Intensity (solid line) and frequency (dashed line) emitted by the OPG as a function of the Fresnel number. This corresponds to an enlargement of Fig. 2. The dashed lines do not result from a fit: they have been added to make the reading of the figure easier.

and the shift of the active detuning interval can lead to a decrease of the emitted intensity. Unfortunately, the theoretical analysis performed until now concerns only monomode cases. To describe more precisely this behavior, it is necessary to use a multimode model. It is not in the scope of this paper to check quantitatively theoretical predictions, but this could be the subject of a future work.

The behavior described above has been observed in any similar situation. In particular, in the case of a similar cavity ( $R_\nu=3$ ), the same behavior occurs when the detuning is chosen at the  $q=2$  family, but shifted in the direction of the  $q=1$  family, or when it is chosen at the  $q=1$  family, and shifted to the  $H_{00}$  mode (Fig. 11).

## V. CONCLUSION

Although OPG exhibit many similarities with lasers, in particular concerning their dynamics, fundamental differences appear in the details of the mechanisms leading to these behaviors, in particular concerning their emission frequency. We have shown in this paper that because of the very narrow bandwidth of the OPG, a very large pulling of the empty cavity modes frequency occurs towards the maximum gain frequency. This pulling has an expression quite different from that encountered in lasers, leading to original behaviors in OPG. We have shown in particular that the frequency pulling is essentially of constant sign, so that the emission frequency of pulled modes is always on the same side as compared to the maximum gain frequency. We also show that the particular properties of the frequency pulling in OPG may lead to paradoxical behavior, as a decreasing of the emitted intensity when the losses are decreased. An open question is now to know what are the consequences of these effects on the oscillator dynamics. If—as we can suppose—they are not negligible, it is necessary to develop more accurate OPG models than the class-A model. A first step could be to make a bimodal model that should help in detailing the interpretations given here: this could be the object of future studies.

## ACKNOWLEDGMENTS

The authors wish to thank P. Glorieux for fruitful discussions. The Laboratoire de Physique des Lasers, Atomes et

Molécules is “Unité Mixte de Recherche de l’Université de Lille 1 et du CNRS” (UMR 8523). The Center d’Etudes et de Recherches Lasers et Applications (CERLA) is supported by the Ministère chargé de la Recherche, the Région Nord-

Pas de Calais, and the Fonds Européen de Développement Economique des Régions. R. Herrero acknowledges support from the CIRIT (Generalitat de Catalunya) for a grant (No. 1995BEAI300257).

- 
- [1] D. Hennequin, L. Dambly, D. Dangoisse, and P. Glorieux, *J. Opt. Soc. Am. B* **11**, 676 (1994).
- [2] J. Farjas, D. Hennequin, D. Dangoisse, and P. Glorieux, *Phys. Rev. A* **57**, 580 (1998).
- [3] F. T. Arecchi, S. Boccaletti, P. L. Ramazza, and S. Residori, *Phys. Rev. Lett.* **70**, 2277 (1993).
- [4] Z. Chen, D. McGee, and N. B. Abraham, *J. Opt. Soc. Am. B* **13**, 1482 (1996).
- [5] J. Malos, M. Vaupel, K. Staliunas, and C. O. Weiss, *Phys. Rev. A* **53**, 3559 (1996).
- [6] D. R. Korwan and G. Indebetouw, *J. Opt. Soc. Am. B* **13**, 1473 (1996).
- [7] See, e.g., papers in *Landmark Papers on Photorefractive Non-linear Optics*, edited by Pochi Yeh and Claire Gu (World Scientific, Singapore, 1995).
- [8] K. Staliunas, M. F. H. Tarroja, G. Sleky, C. O. Weiss, and L. Dambly, *Phys. Rev. A* **51**, 4140 (1995).
- [9] L. Dambly and H. Zeghlache, *Phys. Rev. A* **47**, 2264 (1993).
- [10] A. Yariv and S.-K. Kwong, *Opt. Lett.* **10**, 454 (1985).
- [11] S.-K. Kwong, M. Cronin-Golomb, and A. Yariv, *IEEE J. Quantum Electron.* **QE-22**, 1508 (1986).